G. Bertoni et al. Ultramicroscopy 106 (2006) 630-635

Quantification of crystalline and amorphous content in porous TiO_2 samples from electron energy loss spectroscopy

G. Bertoni[a,*], E. Beyers[b], J. Verbeeck[a], M. Mertens[c], P. Cool[b], E.F. Vansant[b], G. Van Tendeloo[a]

[a]*Electron Microscopy for Materials Science (EMAT), University of Antwerp, Groenenborgerlaan 171, B-2020 Antwerp, Belgium*
[b]*Laboratory of Adsorption and Catalysis, University of Antwerp, Universiteitsplein 1, B-2160 Antwerp, Belgium*
[c]*Flemish Institute for Technological Research (VITO), Boerentang 200, B-2400 Mol, Belgium*

Abstract

We present an efficient method for the quantification of crystalline versus amorphous phase content in mesoporous materials, making use of electron energy loss spectroscopy. The method is based on fitting a superposition of core-loss edges using the maximum likelihood method with measured reference spectra. We apply the method to mesoporous TiO_2 samples. We show that the absolute amount of the crystalline phase can be determined with an accuracy below 5%. This method takes also the amorphous phase into account, where standard X-ray diffraction is only quantitative for crystalline phases and not for amorphous phase.

PACS: 79.20.Ux; 82.80.Pv; 02.60.Ed; 61.66.Fn

Keywords: EELS; Quantification; Mesoporous materials

---

1. Introduction

Titania has been studied extensively because of its wide applications as sensor [1,2], solar cell [3–5], or photocatalyst [6,7]. Of the three crystalline titania phases, anatase is investigated most, for its semi-conducting possibilities and its photo-catalytic activity. Anatase can be used to decolorise wastewater [8,9], or for the oxidation of organic compounds [10,11]. The catalytic activity of a titania sample depends consequently on the amount of anatase present in the sample, with respect to other possibly amorphous titania phases. In literature, most of the times the amount of crystalline phases is determined with Raman measurements or X-ray diffraction (XRD). Raman can only give qualitative information about the crystalline phases, but it does not give any information about the proportions of the different phases. XRD can be used quantitatively: the weight fractions of the different crystalline phases can be calculated from the integrated intensities of the anatase (1 0 1), rutile (1 1 0), and brookite (1 2 1) peaks [12]. This method is often used to determine the proportion of anatase versus rutile, but does not take into account the amount of amorphous titania [13,14]. Most of the times, the amorphous content of the sample is simply not discussed. A technique was developed by Yanagisawa et al. [15] to determine the amount of anatase, considering also the amorphous content. Anatase nanoparticles were formed by hot-pressing of amorphous titania particles, leading to a incomplete crystallization. The amount of anatase was determined by comparison of the density of the bulk material with the theoretical density of anatase. However, this method cannot be used for all titania materials, consisting of crystalline and amorphous titania. The method is not useful when the structure of the material influences the density of the crystalline phase. This is the case of porous materials. Porous titania consists of a network, with pores inside its structure. The size of these pores determines if the material is called micro-, meso- or

---

[*] Corresponding author. Tel.: +32 32653472; fax: +32 32653257.
E-mail address: Giovanni.Bertoni@ua.ac.be (G. Bertoni).
URL: http://webhost.ua.ac.be/emat/.

macro-porous. Following the IUPAC classification, materials with a pore diameter less than 2 nm are micro-porous. Meso-porous materials have pore diameters between 2 and 50 nm and the diameter of macro-pores is larger than 50 nm.

In this study electron energy loss spectroscopy (EELS) was used for the first time to characterize the anatase versus amorphous content in mesoporous titania. In the EELS process incident electrons are inelastically scattered passing through the sample, losing energy. A core electron of the sample can be promoted to unoccupied states (core-loss process). The corresponding core edge (the titanium $L_{2,3}$ edge in our case) in the spectrum carries information about the electronic structure and symmetry (coordination) of the corresponding excited atom. This fine structure can be used to identify different components and phases. This approach does not suffer from the limitation of diffraction techniques, because the density of the materials influences negligibly the shape of the spectra, and can be used to quantify also porous materials. Different techniques have been developed to extract components from an EELS spectrum, based on fitting procedures.

Müllejans and Bruley have developed a so-called spatial difference analysis [16], used in the study of interfaces [17,18]. In this technique the spectra of the core edge of interest are acquired at the interface and far from the interface. Then the spectra far from the interface (or reference spectra) are subtracted from the spectrum at the interface to give a difference spectrum (spatial difference). An unknown component at the interface can be extracted in this way. However, a scaling of the references spectra is necessary before subtraction, introducing unknown variables (the scaling factors). Further hypothesis have to be introduced to solve the problem. Often the reference spectra are scaled opportunely to minimize the difference spectrum but avoiding negative points [17,18]. Of course, in this way, only the lower limit for the amount of the unknown component can be estimated.

Another technique is based on principal components analysis. We do not enter into details, and we refer the reader to Ref. [19]. The unknown component can be extracted from a set of EELS spectra. Also in this case, the approach works well for an interface between two materials, but becomes complicated in a mixing of two phases with unknown amounts. Only a big set of spectra corresponding to different concentration ratios of the two phases can converge and give out the shape of the two components.

To solve our problem, we need to know the shape of the edges for two components (anatase and amorphous titania in this case). So we need to measure experimentally the Ti $L_{2,3}$ spectrum from a pure anatase sample, and from an amorphous titania sample. A maximum likelihood (ML) fitting procedure can then give the resulting concentrations for the two components in a mixed sample, assuming that the acquired spectrum is a pure superposition of the two constituent spectra.

2. Experimental

For the synthesis of mesoporous titania and the amorphous phase, hexadecylamine (HDA; Acros 90%) or pluronic P123 ($EO_{20}PO_{70}EO_{20}$, Sigma-Aldrich) was used as surfactant, while titanium tetra-isopropoxide ($Ti(O^{i}Pr)_4$; Aldrich 97%) was used as titanium source.

For the EELS measurements reference spectra were needed from anatase and amorphous phase. Anatase is commercially available, but this is not the case for amorphous titania. An amorphous phase was synthesized by the following procedure (sample A). After dissolution of HDA in EtOH (Acros pro analysis grade) $Ti(O^{i}Pr)_4$ was added and stirred at ambient temperature. After a drop wise addition of water to this solution, a white suspension was formed and the mixture was stirred during 15 min. The solution was aged during 24 h at room temperature in a closed system to avoid evaporation. The molar gel composition was $Ti:HDA:H_2O:EtOH = 1:0.33:2:90$. After 24 h aging, the mixture was transferred into a Petri dish for 7 days at room temperature to evaporate the solvent. The sample was further treated with NH_4OH (Acros 28–30% p.a.) for 48 h in a reflux system. One gram of solid was treated with 50 ml of basic water. The pH was kept constant between a value of 9 and 10, by the addition of NH_4OH.

Two mesoporous titania samples (B and C), containing mixtures of anatase and amorphous phases, were synthesized. Sample B was synthesized similarly to the amorphous phase, but the HDA surfactant was removed by calcination, during 2 h at 300 °C in a tube furnace, under air flow. During this thermal treatment, the amorphous titania partly crystallizes into anatase. Sample C was synthesized following the method of Kartini et al. [20]. This synthesis method consists of two steps. First, the formation of the anatase seeds: 5 ml $Ti(O^{i}Pr)_4$ was diluted with 8.3 ml EtOH. This ethanolic titanium solution was added drop wise into a mixture of 6.67 ml H_2O and 1.65 ml EtOH. The solution was stirred during 2 h at room temperature. After this hydrolysis, the suspension was transferred into a Teflon-lined autoclave for thermal treatment at 80 °C for 4 h. In the second step a mesoporous structure was formed from the anatase seeds. The block copolymer P123 ($EO_{20}PO_{70}EO_{20}$) was used as surfactant: 3.2 g of surfactant was dissolved in 40 ml water. The seed solution was quenched directly after 4 h and added drop wise into the surfactant solution. The resultant mixture was stirred for 1 h at 40–50 °C. Thereafter, the solution was transferred into a Teflon-lined autoclave for thermal treatment at 100 °C for 20 h. The resultant powder was recovered by filtration. To increase the stability of the material, the sample was treated with NH_4OH during 48 h at pH 9–10. Finally, the sample was calcined resulting in a surfactant-free mesoporous material.

FT-Raman was used to determine the crystal phases of the reference materials. Samples were measured on a Nicolet Nexus 670 bench equipped with a Ge detector in a

180° reflective sampling configuration using a 1064 nm Nd:YAG laser.

For all the samples, the EELS spectra were collected with a Philips CM30 transmission electron microscope (TEM), equipped with a field emission gun (FEG) and a Gatan GIF 2000 spectrometer. The images and the electron diffraction (ED) patterns were collected on a Gatan 2k × 2k camera. The spectra were acquired in diffraction mode, and the beam convergence semi-angle and spectrometer acceptance semi-angle were carefully measured, resulting in a total collection angle between 2.7 and 3.0 mrad for all the measurements. The extraction voltage of the gun was reduced to 2.54 kV to increase the energy resolution. This was measured from the full-width at half-maximum (FWHM) of the zero-loss peak to be 0.8 eV in all sets of acquisitions. The fits were performed with EELSMODEL [21], a program that makes use of the ML estimator to fit a model to an experimental spectrum, assuming Poisson noise statistics. The output of the program is not only the estimated parameters, but also the statistical quality of the model and the estimated errors on the parameters [22,23].

3. Results and discussion

As we discussed in the Introduction, we need reference spectra for the two components, the crystalline phase (anatase) and the amorphous TiO_2 phase. The Raman spectra of the two phases are shown in Fig. 1 and confirm the purity of the phases.

We verified that the anatase reference sample was composed of big crystal particles (50–200 nm in diameter). This sample was assigned as the reference for completely crystalline TiO_2 phase (100% crystalline).

In Fig. 2 we show the TEM images for the TiO_2 sample A, together with its corresponding ED pattern. As can be seen, sample A does not show evidences of crystal grains formation in the image, and also the ED pattern shows a diffuse background and no points corresponding to crystal planes. We considered this sample as the reference for completely amorphous titania sample (0% crystalline).

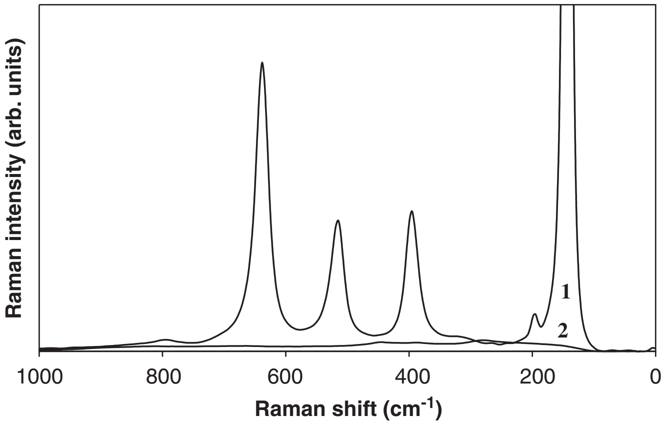

Fig. 1. Raman spectra of commercially available anatase (1) and synthesized amorphous TiO_2 sample A (2).

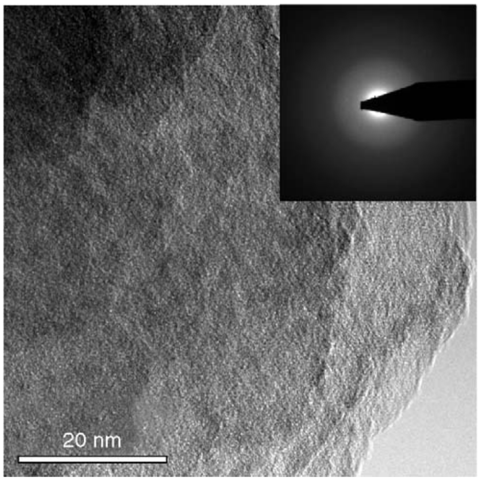

Fig. 2. TEM image from the TiO_2 sample A. No evidence of crystal grains was detected on the sample, as confirmed by the ED pattern (inset). We considered sample A as a TiO_2 amorphous reference.

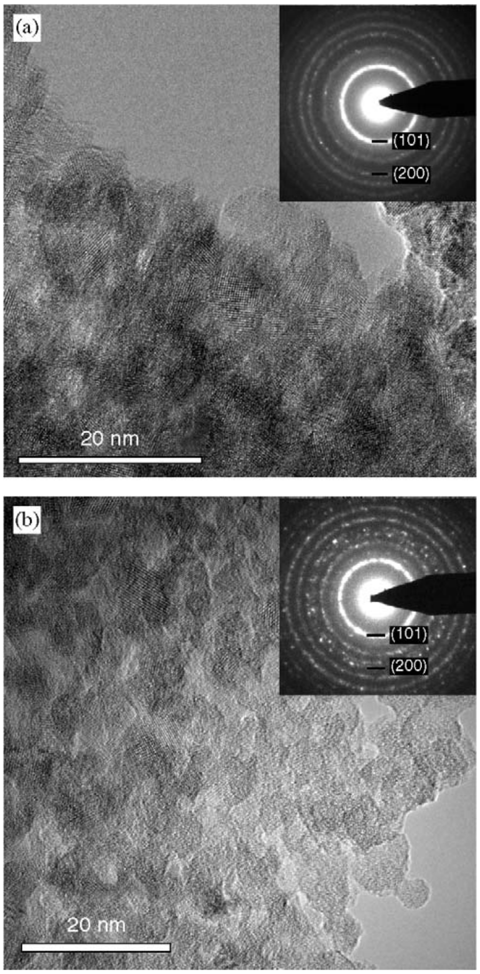

Fig. 3. TEM image from TiO_2 sample B (a), and from TiO_2 sample C (b). The corresponding ED patterns are shown in the insets.

In Fig. 3 the TEM images and ED patterns from samples B and C are shown. Both the samples show the presence of crystal grains (5–10 nm in size). The degree of crystallinity seems higher for C with respect to B. From a careful inspection of the diffraction patterns we found a low intensity from a ring at about 2.9 Å (better visible in sample C). This corresponds to (1 2 1) planes in brookite. The result was confirmed by XRD. The amount of brookite was estimated from XRD to be less than 10% of the total crystalline amount. No detectable traces of rutile phase were found by indexing the ED patterns.

To quantify the amount of crystalline and amorphous phases, we collected EELS spectra from the Ti $L_{2,3}$ edge. The spectra, after background removal and deconvolution, are shown in Fig. 4a. Common to all the spectra is the spin–orbit splitting into $2p_{3/2}$ (L_3) and $2p_{1/2}$ (L_2) levels, with a separation of 5.4 eV [24]. The degree of crystallinity is reflected by the further splitting of the L_2 and L_3 peaks into two peaks due to the crystal-field interaction. The octahedral coordination of titanium atoms with oxygen splits the Ti 3d states into the t_{2g} ($3d_\pi$) and e_g ($3d_\sigma$) symmetries [24]. The asymmetry visible in the spectra from sample A indicates that local octahedral coordination is weakly present also in the amorphous phase. A similar spitting can be observed in the oxygen K edge (Fig. 4b), corresponding to transition to O 2p-Ti 3d hybridized states of t_{2g} and e_g symmetry. Due to the superposition of many different grain orientations in the area illuminated by the beam in the EELS acquisition, orientation effect in the spectra do not need to be taken into account, and the scattering can be considered isotropic.

To perform the fits for the Ti $L_{2,3}$ edge from samples B and C we used the EELSMODEL program [21]. The model to be fitted is composed by a power-law background AE^{-r}, where E is the energy loss and A and r are two parameters to be estimated. Then the two edges from anatase and amorphous phase were added to the background. Finally, the model was convolved with a low-loss spectrum from the same region of the sample, to take into account the effect of multiple scattering processes. More details on creating a model to use for fitting procedure of an EELS experiment can be found in literature [22,23]. The two reference spectra for the anatase and the amorphous TiO_2 were derived from the experimental curves of Fig. 4a. To obtain the correct shape of the edges, an initial deconvolution of the acquired spectra was done, using the standard Fourier ratio method [25] commonly used for core-loss edge spectra, with a Gaussian modifier of 0.8 eV. With this method, the effect of the plural scattering is removed, reducing drastically the difference in the spectra due to different thicknesses. The broadening due to finite resolution of the spectrometer is also partially removed, approaching the natural width of the edge (due to the life-time of the excitation). However, despite these advantages, noise at high frequencies is introduced. This does not constitute a problem in the fitting procedure, due to the final convolution of the total curve with the low-loss spectrum (see Fig. 5). The two reference spectra were normalized in the same energy interval (455–485 eV). The energy window is sufficient to cover the extension of the high-density part of the Ti d-bands. At higher energies, the spectra are almost flat and do not show significant differences due to the structure [27]. The constructed model was fitted using the ML method. This method can be shown to be unbiased and most precise [22], in the assumption of Poisson distributed noise, and if a statistically valid model can be constructed. The only free parameters in the fit are the two parameters A and r for

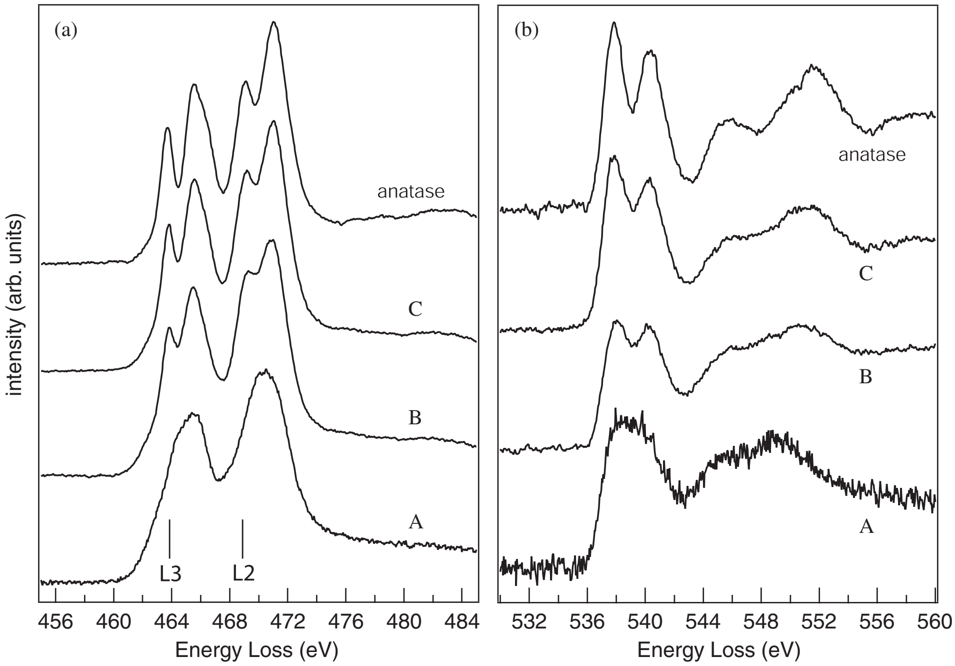

Fig. 4. Titanium $L_{2,3}$ core-Loss (a) and oxygen K core-Loss (b) EELS spectra from the different TiO_2 samples investigated. The spectra are normalized to the same integrated intensity area for Ti and O, respectively.

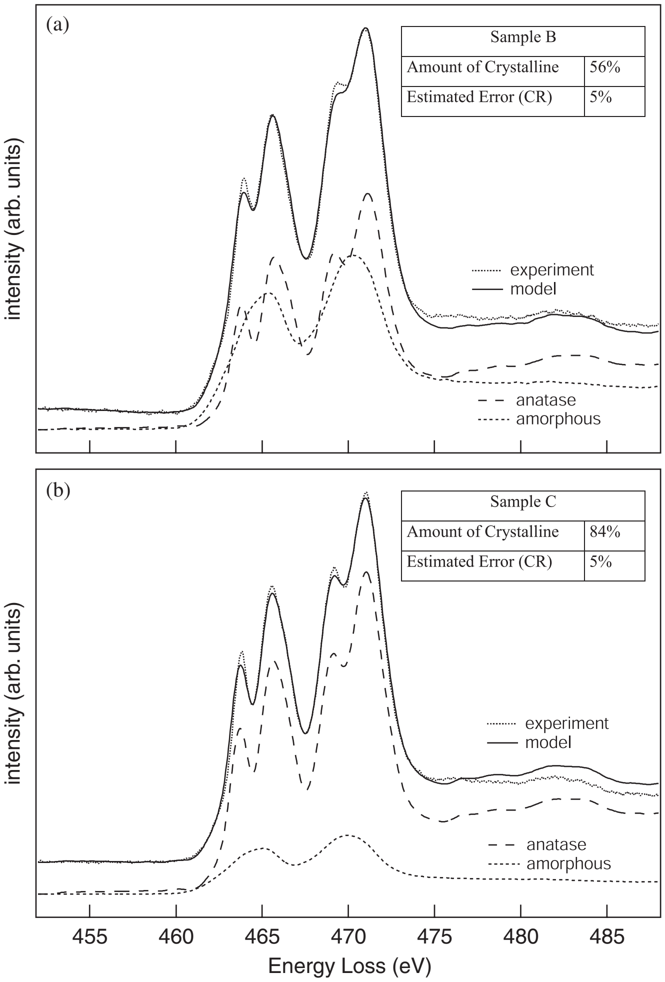

Fig. 5. Results of the fits of the Ti $L_{2,3}$ edges the TiO_2 sample B (a) and TiO_2 sample C (b). In both cases, the experimental spectrum is shown (dots) together with the model after fitting (line). The reference spectra for anatase (dashed line) and amorphous (dotted line) TiO_2, as obtained from the spectra of Fig. 4a, are shown with their scaling factors resulting from the fitting procedure. The amount of crystalline phase is shown in the tables together with the estimated error from the Cramér–Rao lower bound.

the background, and the two scaling factors of the two references. The scaling factors estimates give the amounts of crystalline and amorphous phases, and also the error in their concentrations can be evaluated, as resulting from the Cramér–Rao lower bound [22]. The reference spectra were aligned in energy to the Ti L_3 edge onset in the anatase sample. The two edge onsets positions of the references can also be optimized in the fitting procedure. However, in all the fits we obtained energy differences in the crystalline and amorphous edge onsets less than 0.6 eV. For average purposes, we illuminated the samples over an area of several hundreds square nanometers (around 900 nm^2). We considered the measurements from the illuminated areas representative of the samples, with the estimated errors in the crystalline to amorphous ratios from the Cramér–Rao lower bound. The resulting curves from the fits are shown in Fig. 5, together with the estimations for the amount of the crystalline phase. The estimated error from the Cramér–Rao lower bound results are found to be close to 5%. In summary, sample B shows a percentage of crystallinity of 56%, while sample C is highly crystalline, around 85% in average. Of course, these values are relative to the commercial anatase used as reference TiO_2. We want to note that the error in the measurements can be higher than the statistical error in the case of not spatially homogeneous samples. The measurement can be in that case repeated in different regions of the sample to obtain an average value of the ratio crystalline/amorphous with its statistical standard deviation. TEM is powerful for local information, but lacks average quantification information on the micron or millimeters scale, unless collecting a big amount of data from different points on the samples. A valid alternative in this case is to apply the same approach to soft X-ray absorption techniques (NEXAFS spectroscopy), collecting the drain current or the fluorescent X-ray yield from the sample [28]. The technique is formally identical to EELS (the photon polarization in NEXAFS plays the role of the scattering vector in EELS) with the use of bigger lateral dimensions of the probe source.

We have some remarks on the fitting procedure. First, we did not take into account the brookite phase. Effectively, with our energy resolution of 0.8 eV, it is difficult to estimate the relative amount of anatase and brookite, due to the similarities of the Ti $L_{2,3}$ edge for the two phases [24,26], the tiny amount of brookite phase in our samples, and the presence of the amorphous phase. To recognize two different crystalline phases in the spectrum, a better energy resolution would be necessary, e.g. using a monochromator [26]. Second, the statistical acceptance of the fits has to be taken into account. This gives us the probability that the model reproduces the experimental data, and can be calculated from the likelihood merit function [22]. The model is statistically accepted if its confidence level is greater than 95%. In the case of the spectra of Fig. 5, the confidence level is below 95%, which means the model has to be rejected. This is a common problem in statistical cases with low noise and few degrees of freedom [22]. In these cases, also if the confidence level is low, the values of the estimates are very close to the values in the case of accepted models [22,23], within the statistical error from the Cramér–Rao lower bound. The estimates for the amount of crystalline and amorphous content we derived can therefore be used with care. A better model should be built, for example, improving the deconvolution techniques of the reference edges (this can improve the fit at the maxima of the peaks in the spectra). We excluded the presence of a rutile phase in the samples. No rutile was indeed detectable from the ED patterns. Finally, we said that oxygen spectra show a similar trend respect to Ti. However, we do not report results on quantification for oxygen. This come from the fact that the oxygen spectrum for the amorphous reference, taken from the not calcinated sample A, still contains oxygen coming from the surfactant and the template, and not only from pure amorphous TiO_2.

4. Conclusions

We presented in this paper an efficient method of quantification of crystalline and amorphous contents in a sample, making use of EELS core-loss fine structures. The procedure is based on collecting reference spectra, and then fitting the experimental data with the ML estimator. We applied this procedure to mesoporous TiO_2 samples. The crystalline phase was quantified with a statistical error of 5%. The method can be applied to all cases where reference spectra are collectible. A good example is the quantification of graphitic and amorphous contents in carbon films [29].

Acknowledgments

This work has been performed within the IAP-V framework of the Belgian government and the GOA-2005 program. G. Bertoni wants to thank the financial support from the FWO-Vlaanderen under contract G.0425.05.

References

[1] A.M. Ruiz, A. Cornet, K. Shimanoe, J.R. Morante, N. Yamazoe, Sens. Actuator B-Chem. 109 (2001) 7.
[2] N. Savage, B. Chwieroth, A. Ginwalla, B.R. Patton, S.A. Akbar, P.K. Dutta, Sens. Actuator B-Chem. 79 (2001) 17.
[3] Y.-Q. Wang, S.-G. Chen, X.-H. Tang, O. Palchik, A. Zaban, Y. Koltypin, A. Gedanken, J. Mater. Chem. 11 (2001) 521.
[4] M. Grätzel, Curr. Opin. Colloid Interface Sci. 4 (1999) 314.
[5] G. Phani, G. Tulloch, D. Vittorio, I. Skryabin, Renew. Energy 22 (2001) 303.
[6] O. Legrini, E. Oliveros, A.M. Braun, Chem. Rev. 93 (1993) 671.
[7] P.S. Awati, S. V Awate, P.P. Shah, V. Ramaswamy, Catal. Commun. 4 (2003) 393.
[8] M. Sökmen, A. Ozkan, J. Photochem. Photobiol. A-Chem. 147 (2002) 77.
[9] J. Chen, M. Liu, L. Zhang, J. Zhang, L. Jin, Water Res. 37 (2003) 3815.
[10] M. Andersson, L. Osterlund, S. Ljungström, A. Palmqvist, J. Phys. Chem. B 106 (2002) 10647.
[11] T. Ohno, K. Tokieda, S. Higashida, M. Matsumura, Appl. Catal. A-Gen. 244 (2003) 383.
[12] H. Zhang, J.F. Banfield, J. Phys. Chem. B 104 (2000) 3481.
[13] J.C. Yu, L. Zhang, J. Yu, Chem. Mat. 14 (2002) 4647.
[14] M.P. Moret, R. Zallen, D.P. Vijay, S.B. Desu, Thin Solid Films (2000) 1–3.
[15] K. Yanagisawa, K. Ioku, N. Yamasaki, J. Am. Ceram. Soc. 80 5 (1997) 1303.
[16] H. Müllejans, J. Bruley, Ultramicroscopy 53 (1994) 351.
[17] C. Scheu, G. Dehm, H. Müllejan, R. Brydson, M. Rühle, Microsc. Microanal. 6 (1995) 19.
[18] G. Dehm, C. Scheu, G. Möbus, R. Brydson, M. Rühle, Ultramicroscopy 67 (1997) 207.
[19] N. Bonnet, N. Brun, C. Colliex, Ultramicroscopy 77 (1999) 97.
[20] I. Kartini, D. Menzies, D. Blake, J.C.D. da Costa, P. Meredith, J.D. Tiches, G.Q. Lu, J. Mater. Chem. 14 (2004) 2917.
[21] The program is freely available under the GNU public license and it can be downloaded from ⟨http://webhost.ua.ac.be/eelsmod/eelsmodel.htm⟩.
[22] J. Verbeeck, S. Van Aert, Ultramicroscopy 101 (2004) 207.
[23] J. Verbeeck, S. Van Aert, G. Bertoni, Ultramicroscopy, accepted for publication.
[24] M. Okada, P. Jing, Y. Yamada, M. Tazawa, K. Yoshimura, Surf. Sci. 566–568 (2004) 1030.
[25] R.F. Egerton, Electron Energy-Loss Spectroscopy in the Electron Microscope, second ed., Plenum Press, New York, 1996, pp. 262–269.
[26] S. Lazar, G.A. Bottom, M.-Y. Wu, F.D. Tichelaar, H.W. Zandbergen, Ultramicroscopy 96 (2003) 535.
[27] P.L. Potapov, K. Jorissen, D. Schryvers, D. Lamoen, Phys. Rev. B 70 045106 (2004) 1.
[28] J. Stöhr, Nexafs Spectroscopy, first ed., Springer, Berlin, 2003.
[29] J.T. Titantah, D. Lamoen, Phys. Rev. B 70 075115 (2004) 1.